RADC-TR-90-155
Final Technical Report
July 1990

RESONANCE REGION SCATTERING

Syracuse University

Xiaopu Yang and Ercument Arvas

APPROVED FOR PUBLIC RELEASE; DISTRIBUTION UNLIMITED.

Rome Air Development Center
Air Force Systems Command
Griffiss Air Force Base, NY 13441-5700

RADC-TR-90-155 has been reviewed and is approved for publication.

APPROVED:

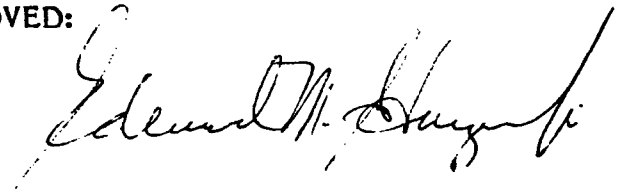

EDWARD M. STARCZEWSKI
Project Engineer

APPROVED:

FRED J. DEMMA, Actg Director
Directorate of Surveillance

FOR THE COMMANDER:

JOHN A. RITZ
Directorate of Plans & Programs

DESTRUCTION NOTICE - For classified documents, follow the procedures in DOD 5200.22-M, Industrial Security Manual, or DOD 5200.1-R, Information Security Program Regulation. For unclassified, limited documents, destroy by any method that will prevent disclosure of contents or reconstruction of the document.

If your address has changed or if you wish to be removed from the RADC mailing list, or if the addressee is no longer employed by your organization, please notify RADC (OCTM), Griffiss AFB NY 13441-5700. This will assist us in maintaining a current mailing list.

Do not return copies of this report unless contractual obligations or notices on a specific document requires that it be returned.

REPORT DOCUMENTATION PAGE

Form Approved OPM No. 0704-0188

1. AGENCY USE ONLY *(Leave Blank)*	2. REPORT DATE	3. REPORT TYPE AND DATES COVERED
	July 1990	Final Jun 89 - Feb 90

4. TITLE AND SUBTITLE

RESONANCE REGION SCATTERING

5. FUNDING NUMBERS

C - F30602-88-D-0027
PE - 63741D
PR - 3640
TA - 04
WU - P1

6. AUTHOR(S)

Xiaopu Yang and Ercument Arvas

7. PERFORMING ORGANIZATION NAME(S) AND ADDRESS(ES)

Syracuse University
Dept of Electrical and Computer Engineering
Syracuse NY 13244

8. PERFORMING ORGANIZATION REPORT NUMBER

N/A

9. SPONSORING/MONITORING AGENCY NAME(S) AND ADDRESS(ES)

Rome Air Development Center (OCTM)
Griffiss AFB NY 13441-5700

10. SPONSORING/MONITORING AGENCY REPORT NUMBER

RADC-TR-90-155

11. SUPPLEMENTARY NOTES

RADC Project Engineer: Edward M. Starczewski/OCTM/(315) 330-4431

12a. DISTRIBUTION/AVAILABILITY STATEMENT

Approved for public release; distribution unlimited.

12b. DISTRIBUTION CODE

13. ABSTRACT *(Maximum 200 words)*

Using frequency derivative information, techniques were developed to predict the scattering from conductor and dielectric 2-D targets over a frequency band. Instead of computing a method of moments solution using a point by point approach, a rational function model is used to approximate the current as a function of frequency. The model coefficients are computed using frequency derivative information at one frequency within the band to improve efficiency of conventional moment method approaches. Results show that the model based approach gives excellent results over a limited frequency band, and is much more efficient than the conventional point by point approach. Keywords:

14. SUBJECT TERMS

Spectral Estimation, Method of Moments,
Frequency Derivatives, Radar Cross Section, (jnd)

15. NUMBER OF PAGES

36

16. PRICE CODE

17. SECURITY CLASSIFICATION OF REPORT	18. SECURITY CLASSIFICATION OF THIS PAGE	19. SECURITY CLASSIFICATION OF ABSTRACT	20. LIMITATION OF ABSTRACT
UNCLASSIFIED	UNCLASSIFIED	UNCLASSIFIED	UL

Use of Frequency-Derivative Information to Compute EM-Scattering from Multiple Perfectly Conducting and Dielectric Cylinders of Arbitrary Cross-Section over a Frequency Band

by Xiaopu Yang

Ercument Arvas

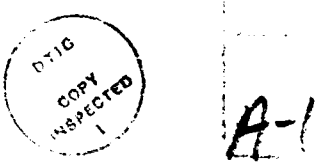

A-1

I. Introduction

The use of frequency-derivative information incorporated with model-based parameter estimation (MBPE) to obtain electromagnetic response of an antenna, propagation path, or a scatterer over a spectrum of frequencies has been studied by a few researchers [1]. In this report, we present some interesting results obtained when the theory is applied to E-field solution of TM-Scattering from multiple perfectly conducting and lossy dielectric cylinders of arbitrary cross-section.

The moment method solution of above mentioned problem has been formulated in [2]. When the solution over a frequency band are required, the method used most often is the one that finds the solution at a set of discrete frequencies, and then interpolates them over the frequency band. The cost of computation for this conventional method can be very high when the number of discrete frequencies is high as it is usually the case to obtain esthetic appearance of low-order interpolatory curve. In contrast, MBPE approach exploits the underlying physics of the phenomenon being modeled so that unnecessary computation is avoided. Using frequency-derivative information further reduces the cost of computation since as far as determination of model coefficients is concerned, frequency-derivative samples bear the same amount of information as frequency samples, but the former are much easier to obtain. Moreover, as demonstrated by numerical results presented in this report, using frequency-derivative information has other advantages, such as better local approximation and easier implementation.

II. Model-Based Parameter Estimation

A. A Rational Function Representation

The MBPE approach utilizes the mathematical property that the frequency response is well approximated by a rational function of form

$$F(s) = N(s)/D(s) = [\sum_{i=0}^{P} N_i s^i]/[\sum_{i=0}^{Q} D_i s^i], \quad (1)$$

which in turn is originated from the Singularity-Expansion Method [3] in using a pole series in complex frequency $s=\sigma+jw$ to model the frequency response, i.e.

$$F(s)= F_p(s)+F_{np}(s) = \sum_{\alpha=1}^{M} R_\alpha/(s-s_\alpha) + \sum_{\beta=-L}^{N} C_\beta s^\beta \quad (2)$$

where $F_{np}(s)$ accounts for the nonpole portion of $F(s)$, and in $F_p(s)$ the parameters R_α and s_α are the residues and corresponding poles. While the number of poles is theoretically infinite to cover the entire frequency band, quite often an approximation to $F(s)$ over a limited frequency band is of interest so that the number of poles used in the model is small, and problem of ill conditioning can be avoided. More models can be used to cover a wider frequency band. In our results, surface currents defined in the method of moments are modeled by a rational function of frequency. For simplicity, unless we mention otherwise, the current is modeled by

$$I(s) = \sum_{\alpha=1}^{P} R_\alpha/(s-s_\alpha)+C_0, \qquad (3)$$

which is equivalent to

$$I(s) = N(s)/D(s) = [\sum_{i=0}^{P} N_i s^i]/[\sum_{i=0}^{P} D_i s^i], \qquad (4)$$

in which there are 2P+1 coefficients N_i's and D_i's to be determined ($D_0=1$).

B. Computing Model Coefficients Using Frequency-Derivative Samples

The coefficients N_i's and D_i's of Eq.(4) can be found when frequency-derivative samples at some frequency ($s=s_0=jw_0$) are available, where w_0 is in the frequency band of interest. Starting with Eq.(4) and differentiating t times with respect to s, there results the following

$$\begin{aligned} &I(s)D(s)=N(s) \\ &I'(s)D(s)+I(s)D'(s)=N'(s) \\ &I''(s)D(s)+2I'(s)D'(s)+I(s)D''(s)=N''(s) \qquad (5) \\ &\cdot \\ &\cdot \\ &\cdot \end{aligned}$$

$$I^{(t)}(s)D(s)+tI^{(t-1)}D'(s)+\ldots+C_{t,t-m}I^{(m)}(s)D^{(t-m)}+$$
$$+\ldots+I(s)D^{(t)}(s)=N^{(t)}(s)$$

where $C_{r,s} = r!/[s!(r-s)!]$ is the binomial coefficient. The system of t+1 equations in Eq.(5) provides the information from which the model coefficients can be found if $t+1 \geq 2P+1$. With no loss of generality, Eq.(5) can be simplified by setting $s_0=0$ with s representing the frequency variation about s_0. We then obtain the following matrix representation for the unknown coefficients

$$\begin{bmatrix} 1 & 0 & \ldots & 0 & 0 & 0 & \ldots & 0 \\ 0 & 1 & \ldots & 0 & -I_0 & 0 & \ldots & 0 \\ 0 & 0 & \ldots & 0 & -I_1 & -I_0 & \ldots & 0 \\ \cdot & & & & \cdot & & & \cdot \\ \cdot & & & & \cdot & & & \cdot \\ 0 & 0 & \ldots & 1 & -I_{P-1} & -I_{P-2} & \ldots & -I_0 \\ 0 & 0 & \ldots & 0 & -I_P & -I_{P-1} & \ldots & -I_1 \\ 0 & & \ldots & 0 & -I_{P+1} & \ldots & & -I_2 \\ \cdot & & & & & & & \\ \cdot & & & & & & & \\ 0 & & \ldots & 0 & -I_{2P-1} & \ldots & & -I_P \end{bmatrix} \begin{bmatrix} N_0 \\ N_1 \\ N_2 \\ \cdot \\ \cdot \\ N_P \\ D_1 \\ D_2 \\ \cdot \\ \cdot \\ D_P \end{bmatrix} = \begin{bmatrix} I_0 \\ I_1 \\ I_2 \\ \cdot \\ \cdot \\ I_P \\ I_{P+1} \\ I_{P+2} \\ \cdot \\ \cdot \\ I_{2P} \end{bmatrix} \quad (6)$$

where $I_m = (1/m!)I^{(m)}(s_0)$.

C. Getting Frequency-Derivative Information from more than one Points.

For purpose of comparison, numerical results are also presented of method using frequency-derivative information from more than one frequency points. Specifically, in two points

frequency derivative method, frequency samples and frequency derivative samples at $s_0 \pm s$ are used to find model coefficients. And in three points frequency derivative method, the informations are taken at s_0 and $s_0 \pm s$.

By following the concept in Sec II.B, we can obtain similar matrix equations for the model coefficients. For example, when frequency samples up to the second order derivatives at two points are used, the matrix equation which determines coefficients in model

$$I(s) = (N_0+N_1 s+N_2 s^2)/(1+D_1 s+D_2 s^2+D_3 s^3) \qquad (7)$$

is

$$\begin{bmatrix} 1 & -s & s^2 & I_0(-s)s & -I_0(-s)s^2 & I_0(-s)s^3 \\ 0 & 1 & -2s & I_1(-s)s- & -I_1(-s)s^2+ & I_1(-s)s^3- \\ & & & -I_0(-s) & +2I_0(-s)s & -3I_0(-s)s^2 \\ 0 & 0 & 1 & I_2(-s)s- & -I_2(-s)s^2+ & I_2(-s)s^3- \\ & & & -I_1(-s) & +2I_1(-s)s- & -3I_1(-s)s^2+ \\ & & & & -I_0(-s) & +3I_0(-s)s \\ 1 & s & s^2 & -I_0(s)s & -I_0(s)s^2 & -I_0(s)s^3 \\ 0 & 1 & 2s & -I_1(s)s- & -I_1(s)s^2- & -I_1(s)s^3- \\ & & & -I_0(s) & -2I_0(s)s & -3I_0(s)s^2 \\ 0 & 0 & 1 & -I_2(s)s- & -I_2(s)s^2- & -I_2(s)s^3- \\ & & & -I_1(s) & -2I_1(s)s- & -3I_1(s)s^2- \\ & & & & -I_0(s) & -3I_0(s)s \end{bmatrix} \begin{bmatrix} N_0 \\ N_1 \\ N_2 \\ D_1 \\ D_2 \\ D_3 \end{bmatrix} = \begin{bmatrix} I_0(-s) \\ I_1(-s) \\ I_2(-s) \\ I_0(s) \\ I_1(s) \\ I_2(s) \end{bmatrix} \qquad (8)$$

where $I_m = (1/m!)I^{(m)}(s_0)$. Similarly, we can find the matrix equation for coefficients of model

$$I(s) = (N_0+N_1s+N_2s^2+N_3s^3+N_4s^4)/(1+D_1s+D_2s^2+D_3s^3+D_4s^4) \quad (9)$$

using information up to the second order derivatives from three points.

III. Computing Frequency Derivatives in A Moment-Method Model

A. The Basic Idea

Overall computation in obtaining frequency-derivative information needed in Eq.(6) can be dramatically reduced from a moment-method model.

On writing the moment-method equations, we have

$$\sum_{j=1}^{N} Z_{ij}I_j = V_i \quad (10)$$

where Z, I, and V are the impedance matrix and the current and voltage vectors. A solution for the current is

$$I_i = \sum_{j=1}^{N} Y_{ij}V_j \quad (11)$$

where matrix Y is the inverse of Z. If we differentiate Eq.(10)

with respect to frequency, we obtain

$$\sum_{j=1}^{N} (Z_{ij}I'_j+Z'_{ij}I_j) = V'_j \qquad (12)$$

from which results the differentiated current

$$I'_i = \sum_{j=1}^{N} Y_{ij}[V'_j-\sum_{k=1}^{N} Z'_{jk}I_k]. \qquad (13)$$

It is seen that the differentiated current requires an additional number of computations beyond those needed for the current proportional to N^2 rather than N^3 that would be required to obtain another frequency sample.

In general, the n'th frequency derivative of the current is given by

$$I_i^{(n)} = \sum_{j=1}^{N} Y_{ij}[V_j^{(n)}-\sum_{m=1}^{N} C_{n,m}(\sum_{k=1}^{N} Z_{jk}^{(m)} I_k^{(n-m)})]. \qquad (14)$$

B. Implementation in the E-field solution of TM-scattering

Following the development in [2], we have the moment equation

$$Z\ I = V \qquad (15)$$

where

$$Z = \begin{bmatrix} Z_{CC} & Z_{CD} & Z_{CM} \\ Z_{DC} & Z_{DD} & Z_{DM} \\ 0 & Z_{MD} & Z_{MM} \end{bmatrix}, \tag{16}$$

$$I = [\ I^C\ I^D\ K^D\ ]^T, \tag{17}$$

and

$$V = [\ V^C\ C^D\ 0\ ]^T \tag{18}$$

are the equivalent impedance matrix and current and voltage vectors, and they are all functions of frequency either through $k_0 (=w\sqrt{\mu\varepsilon_0})$ or $k (=w\sqrt{\mu\varepsilon})$.

It is seen from Eq. (13) that in addition to the impedance matrix, the differentiated impedance matrices are needed in obtaining the differentiated currents. Basically, there are two integrations that are numerically evaluated in forming the impedance matrix. They are

$$A_1 = -k\eta/4 \int H_0^2 (k|\rho-\rho'|)\, dl', \tag{19}$$

and

$$A_2 = -jk/4 \int H_1^{(2)} (k|\rho-\rho'|)\ n_i^d \cdot (\rho-\rho')/|\rho-\rho'|\, dl'. \tag{20}$$

Similarly, the differentiated impedance matrices involve derivatives of those integrals. By taking derivatives of

Eq. (19) and (20) with respect to k and using properties of Hankel function

$$H_0^{(2)\prime}(x) = -H_1^{(2)}(x), \qquad (21)$$

and

$$H_1^{(2)\prime}(x) = H_0^{(2)}(x) - H_1^{(2)}(x)/x, \qquad (22)$$

we obtain

$$dA_1/dk = A_1/k + (k\eta/4)\int |\rho-\rho'| H_1^{(2)}(k|\rho-\rho'|)\,dl', \qquad (23)$$

$$A_1'' = -A_1/k^2 + A_1^2/k + (k\eta/4)\int |\rho-\rho'|^2 H_0^{(2)}()\,dl', \qquad (24)$$

$$A_1^{(3)} = 3A_1/k^3 - 3A_1'/k^2 + 2A_1''/k - (k\eta/4)\int |\rho-\rho'|^3 H_1^{(2)}()\,dl', \qquad (25)$$

$$A_1^{(4)} = -9A_1/k^4 + 9A_1'/k^3 - 5A_1''/k^2 + 2A_1^{(3)}/k - (k\eta/4)\int |\rho-\rho'|^4 H_0^{(2)}()\,dl', \qquad (26)$$

$$A_1^{(5)} = 45A_1/k^5 - 45A_1'/k^4 + 24A_1''/k^3 - 9A_1^{(3)}/k^2 + 3A_1^{(4)}/k + (k\eta/4)\int |\rho-\rho'|^5 H_1^{(2)}()\,dl', \qquad (27)$$

$$A_1^{(6)} = -225A_1/k^6+225A_1'/k^5-127A_1''/k^4+42A_1^{(3)}/k^3-$$
$$-12A_1^{(4)}/k^2+3A_1^{(3)}/k+$$
$$+(k\eta/4)\int|\rho-\rho'|^6 H_0^{(2)}()\,dl', \qquad (28)$$

$$A_1^{(7)} = 1575A_1/k^7-1575A_1'/k^6+810A_1''/k^5-285A_1^{(3)}/k^4+$$
$$+78A_1^{(4)}/k^3-18A_1^{(5)}/k^2+4A_1^{(6)}/k-$$
$$-(k\eta/4)\int|\rho-\rho'|^7 H_1^{(2)}()\,dl', \qquad (29)$$

$$A_1^{(8)} = -11025A_1/k^8+11025A_1'/k^7-5625A_1''/k^6+$$
$$2950A_1^{(3)}/k^5-519A_1^{(4)}/k^4+114A_1^{(5)}/k^3-$$
$$-22A_1^{(6)}/k^2+4A_1^{(7)}/k-$$
$$-(k\eta/4)\int|\rho-\rho'|^8 H_0^{(2)}()\,dl', \qquad (30)$$

$$dA_2/dk = -jk/4\int H_0^{(2)}(k|\rho-\rho'|)\,n_i^d\cdot(\rho-\rho')\,dl', \qquad (31)$$

$$A_2'' = A_2'+(jk/4)\int H_1^{(2)}()\,[n_i^d\cdot(\rho-\rho')]\,|\rho-\rho'|\,dl', \qquad (32)$$

$$A_2^{(3)} = -A_2'/k^2+A^{2''}/k+$$
$$+(jk/4)\int H_0^{(2)}()\,[n_i^d\cdot(\rho-\rho')]\,|\rho-\rho'|^2 dl', \qquad (33)$$

$$A_2^{(4)} = 3A_2'/k^3-3A_2''/k^2+2A_2^{(3)}/k-$$
$$-(jk/4)\int H_1^{(2)}()\,[n_i^d\cdot(\rho-\rho')]\,|\rho-\rho'|^3 dl', \qquad (34)$$

$$A_2^{(5)} = -9A_2'/k^4+9A_2''/k^3-5A_2^{(3)}/k^2+2A_2^{(4)}/k-$$
$$-(jk/4)\int H_0^{(2)}()\,[n_i^d\cdot(\rho-\rho')]\,|\rho-\rho'|^4 dl', \qquad (35)$$

$$A_2^{(6)} = 45A_2'/k^5 - 45A_2''/k^4 + 24A_2^{(3)}/k^3 - 9A_2^{(4)}/k^2 + 3A_2^{(5)}/k + (jk/4)\int H_1^{(2)}()[n_i^d \cdot (\rho-\rho')]\,|\rho-\rho'|^5 dl', \quad (36)$$

$$A_2^{(7)} = -225A_2'/k^6 + 225A_2''/k^5 - 117A_2^{(3)}/k^4 + 42A_2^{(4)}/k^3 - 12A_2^{(5)}/k^2 + 3A_2^{(6)}/k - (jk/4)\int H_0^{(2)}()[n_i^d \cdot (\rho-\rho')]\,|\rho-\rho'|^6 dl', \quad (37)$$

$$A_2^{(8)} = 1575A_2'/k^7 - 1575A_2''/k^6 + 810A_2^{(3)}/k^5 - 285A_2^{(4)}/k^4 + 78A_2^{(5)}/k^3 - 18A_2^{(6)}/k^2 + 4A_2^{(7)}/k + (jk/4)\int H_1^{(2)}()[n_i^d \cdot (\rho-\rho')]\,|\rho-\rho'|^7 dl'. \quad (38)$$

Using Eq.(23)-(38), the differentiated impedance matrices take the form

$$Z' = \begin{bmatrix} Z'_{CC} & Z'_{CD} & Z'_{CM} \\ Z'_{DC} & Z'_{DD} & Z'_{DM} \\ 0 & Z'_{MD}\varepsilon & Z'_{MM}\varepsilon \end{bmatrix}, \quad (39)$$

$$Z'' = \begin{bmatrix} Z''_{CC} & Z''_{CD} & Z''_{CM} \\ Z''_{DC} & Z''_{DD} & Z''_{DM} \\ 0 & Z''_{MD}\varepsilon^2 & Z''_{MM}\varepsilon^2 \end{bmatrix}, \quad (40)$$

etc., where ε is dielectric constant of the dielectric body.

IV. Sample Numerical Results

Included in this section are sample results obtained from a Fortran computer code which implements the theory presented above. Specifically, the frequency derivative method (FD) is

compared with conventional point by point method (CV) in obtaining the backscattering cross-section (BSCS) of various structures over a frequency band.

Fig.(1) shows the BSCS of a conducting cylinder over a frequency band from $k=0.5k_0$ to $k=2k_0$, where k is wave constant, and k_0 corresponds to the frequency at which frequency derivative samples are taken. There are two curves for FD method. One uses frequency derivative samples up to 4th order, another up to 6th order. It is seen that the curve for 6th order FD method is in excellent agreement with that of CV over entire frequency band of interest, while the curve for 4th order FD method starts deviating around $k=1.7k_0$.

Fig.(2) shows the BSCS of a dielectric cylinder ($\varepsilon_r=4$) of rectangular cross-section. The dimensions of the cylinder and the number of sections approximating the surface in applying moment method are given in the inset of the figure. The observation is similar to that of Fig.(1).

Consider a combination of conductor and dielectric cylinders as shown in Fig.(3). The curves of BSCS for FD method are in fairly good agreement with that of CV method within the neighborhood of k_0 ($k=0.8k_0$ to $k=1.2k_0$). The 6th order FD method gives better approximation than the 4th order FD within frequency band from $k=0.68k_0$ to $k=1.28k_0$.

An interesting example is the BSCS for an empty circular cylinder with an opening $\emptyset_0=5°$. The curve for CV method is presented in [4]. There are two resonances within frequency band from ka=4 to ka=6, where a is the radius of the cylinder. Fig.(4) shows the curves for FD method with frequency derivative samples taken at ka=5 ($k_0a=5$) along with that for CV method. The FD method of 4th, 6th, and 8th order are used. All three curves of FD method locate the resonance around ka=5.16. Notice that the higher the order of FD method, the better its curve agrees with CV curve. In particular, the 4th order curve misses the resonance at ka=5.55 completely, while the 6th order curve gives some indication of resonance there, and the 8th order curve locates the resonance. Next, we take frequency derivative samples at ka=5.3 ($k_0a=5.3$). Then as shown in Fig.(5), all three curve of FD are able to pick up the existing two resonances. However, only 8th order FD curve is in excellent agreement with the CV curve. Finally, several models are used to cover a frequency band from ka=0.6 to ka=6.6. Specifically, entire frequency section is divided into subsections of equal size, and the solution in each section is modeled by a rational function whose coefficients are determined using 6th order FD method. For instance, frequency derivative samples taken at ka=0.8 are used to cover the region from ka=0.6 to ka=1.0, samples taken at ka=1.2 are used to cover ka=1.0 to ka=1.4, and so on. The combined result of those

models are shown in Fig.(6) which gives the same locations of resonance as given in Fig.8(b) of [4].

Fig.(7) shows the result using two points FD method for the same structure used by Fig.(4)-(6). Informations used to determine model coefficients are taken at $ka = k_0a \pm \delta ka$, where $k_0a = 5.0$. Curves corresponding to different δka are shown. It is shown that the curve varies with δka. As far as frequency band from ka=4. to ka=6. is concerned, except the curve with $\delta ka=0.8$, all three other curves indicate both resonances at ka=5.16 and ka=5.55.

Fig.(8) shows the result using three points FD method. The informations are taken at $ka = k_0a$, and $ka = k_0a \pm \delta ka$, where k_0a is again 5.0. Among curves corresponding to four different δka, the one with $\delta ka = 0.3$ gives the best result. In addition to existing resonances, other curves show signs of resonances that are not existing.

Finally, Fig.(9) and Fig.(10) demonstrate the effect of using models other than those given by Eq. (3) and (4). What shown are results of 6th order FD method applied to previous examples with different models. Models are different in orders of polynomials in its numerator and denominator. In both figures, NN is the order of numerator, and ND is the order of denomenator. It is seen that curves corresponding to different

models are different, but they all agree with each other locally around the point where informations are taken.

V. Summary and Conclusions

The problem considered here is that of computing the electromagnetic parameters over a frequency band. Instead of using a point by point approach, a rational function model is used to approximate the parameter of interest as a function of frequency. The model coefficients are computed using frequency derivative information at one frequency within the band to improve efficiency. Sample results are presented which illustrate that the model based approach gives excellent result over a limited frequency band, and is much more efficient than conventional point by point approach.

We have the following conclusions:

First, around the point where frequency sample and its derivatives are taken, there is always a frequency band in which the FD method gives good approximation to the true value of the frequency response. The higher the order of derivatives used, the larger the size of this frequency band. When the same order of derivatives is used, the size of this band still varies from problem to problem. It depends on complexity of the

function to be modeled, i.e. the difference between the order of the assumed rational function model and the order of rational function with complete fitting to the function.

Secondly, one point FD is preferred to multi-point FD for the following reasons. One point FD is simpler to implement in that it involves a matrix equation, Eq.(6), which can be constructed easily, and there is no need to select separation of points as required in multi-points FD; One point FD gives better approximation locally, and separate models can be used when a broad frequency band is of interest.

Finally, when the sum of orders in numerator and denomenator polynomials is fixed, different combination of orders generally yields different result. The selection of the best model requires prior knowledge of the function to be modeled. When such knowledge is not available, model of Eq. (4) is recommended for its simplicity.

References:

[1] Miller, E.K., Use of Frequency-derivative information to reconstruct an electromagnetic transfer function, Private Communication.

[2] Arvas, E., Rao, S.M., and Sarkar, T.K., E-field solution TM-scattering from multiple perfectly conducting and lossy dielectric cylinders of arbitrary cross-section, IEE Proceedings, Vol.133, Pt.H, No.2, April 1986.

[3] Baum, C.E., The singularity expansion method, Chapter 3 in Transient Electromagnetic Fields, Ed. L.F.Felsen, Springer-Verlag, New York.

[4] Arvas, E., Electromagnetic penetration into a dielectric-filled conducting shell of arbitrary cross section through an infinite slot: TM case, Archiv for Electronics and Communication, Vol.42, No.3, May-June, 1988.

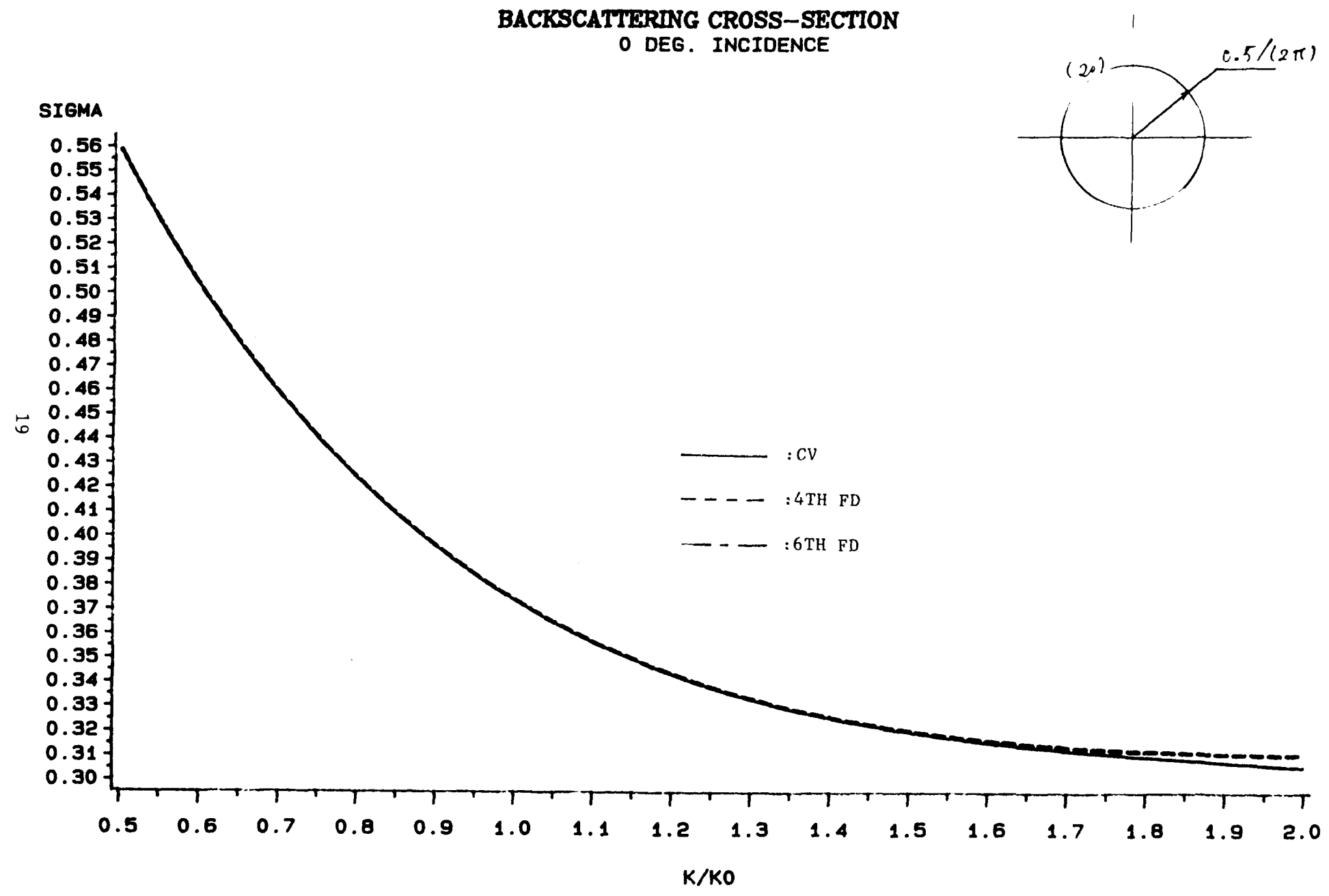
BACKSCATTERING CROSS-SECTION
0 DEG. INCIDENCE
SIGMA
0.56
0.55
0.54
0.53
0.52
0.51
0.50
0.49
0.48
0.47
0.46
0.45
0.44
0.43
0.42
0.41
0.40
0.39
0.38
0.37
0.36
0.35
0.34
0.33
0.32
0.31
0.30
0.5 0.6 0.7 0.8 0.9 1.0 1.1 1.2 1.3 1.4 1.5 1.6 1.7 1.8 1.9 2.0
K/K0
:CV
:4TH FD
:6TH FD
(2ρ)
0.5/(2π)

FIGURE (1)

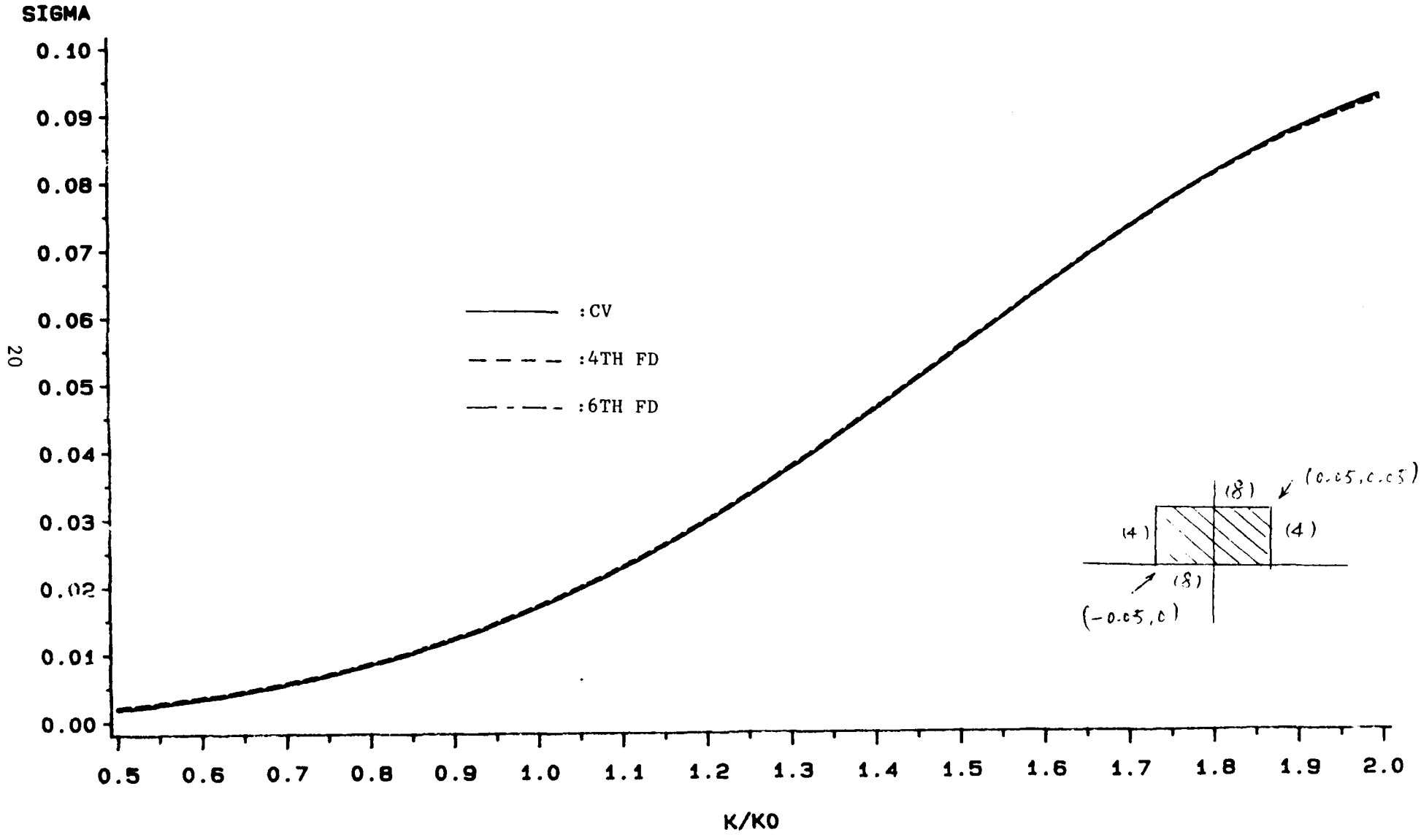
BACKSCATTERING CROSS-SECTION
0 DEG. INCIDENCE
SIGMA
0.10
0.09
0.08
0.07
0.06
0.05
0.04
0.03
0.02
0.01
0.00
20
:CV
:4TH FD
:6TH FD
(8)
(0.05,0.05)
(4)
(4)
(8)
(-0.05,0)
0.5
0.6
0.7
0.8
0.9
1.0
1.1
1.2
1.3
1.4
1.5
1.6
1.7
1.8
1.9
2.0
K/K0

FIGURE (2)

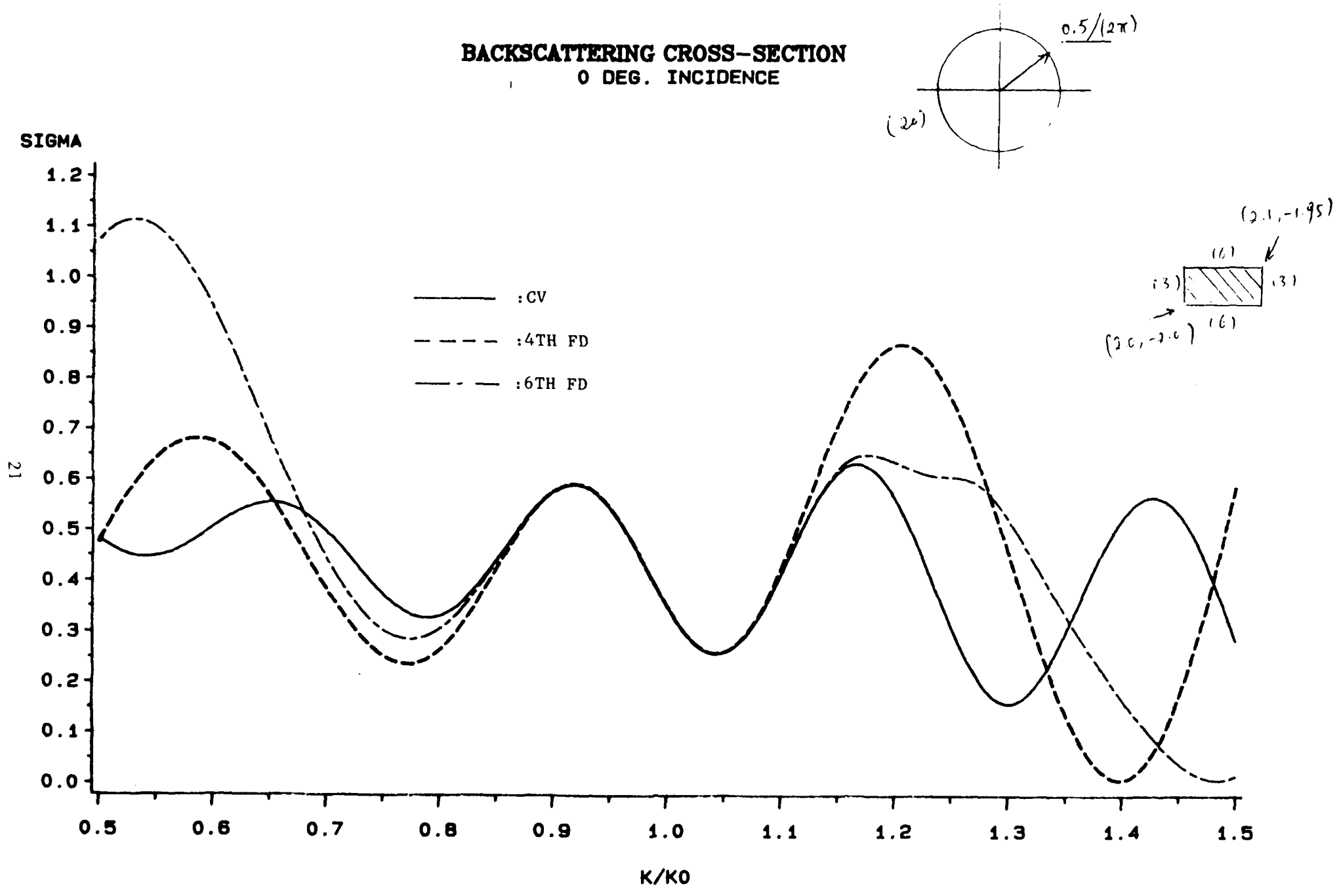
BACKSCATTERING CROSS-SECTION
0 DEG. INCIDENCE
SIGMA
1.2
1.1
1.0
0.9
0.8
0.7
0.6
0.5
0.4
0.3
0.2
0.1
0.0
:CV
:4TH FD
:6TH FD
0.5
0.6
0.7
0.8
0.9
1.0
1.1
1.2
1.3
1.4
1.5
K/KO
0.5/(2π)
(20)
(2.1,-1.95)
(6)
(3)
(3)
(6)
(2.0,-2.0)

FIGURE (3)

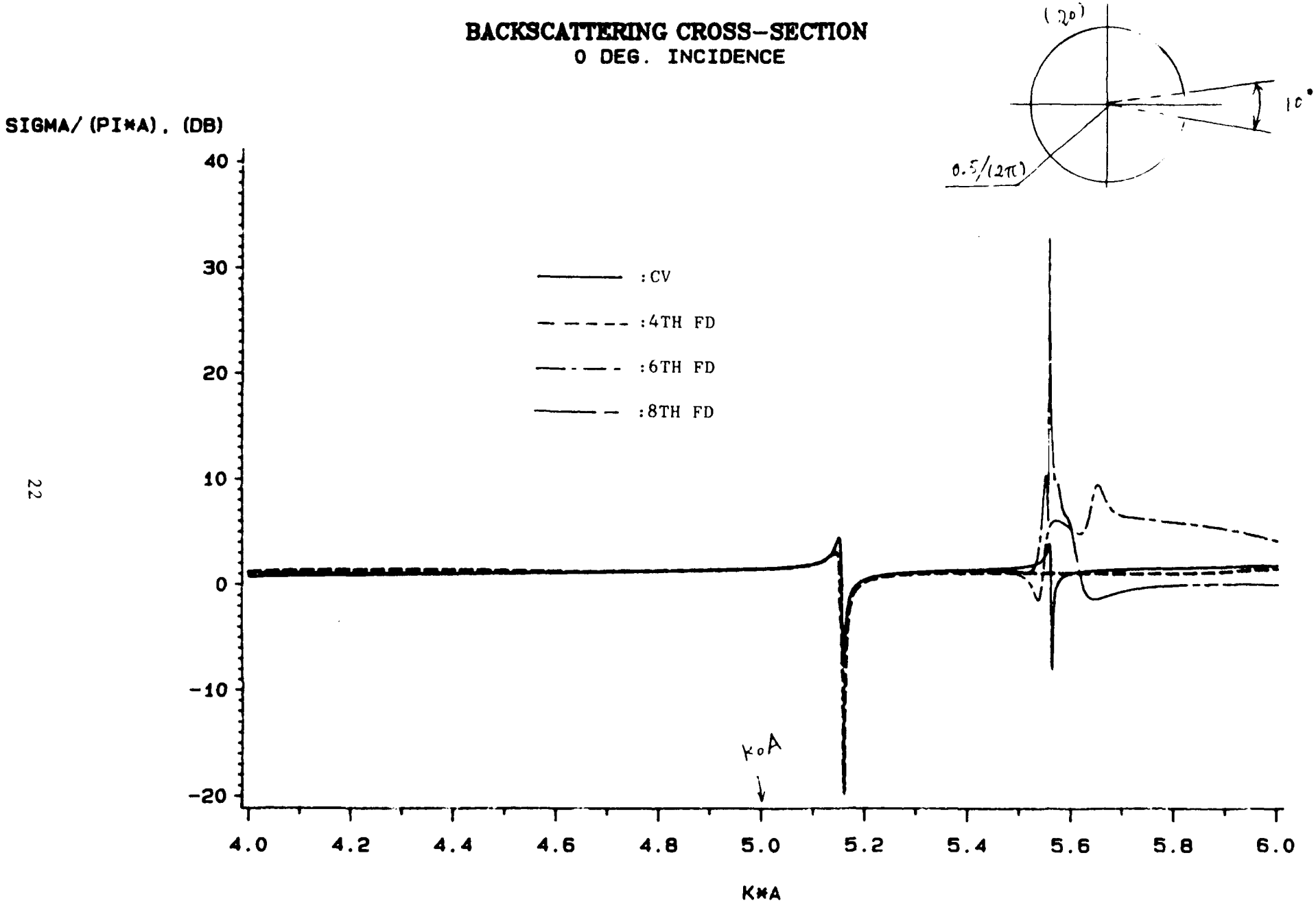
BACKSCATTERING CROSS-SECTION
0 DEG. INCIDENCE
SIGMA/(PI*A). (DB)
40
30
20
10
0
-10
-20
4.0
4.2
4.4
4.6
4.8
5.0
5.2
5.4
5.6
5.8
6.0
K*A
:CV
:4TH FD
:6TH FD
:8TH FD
K₀A
(20)
10°
0.5/(2π)

FIGURE (4)

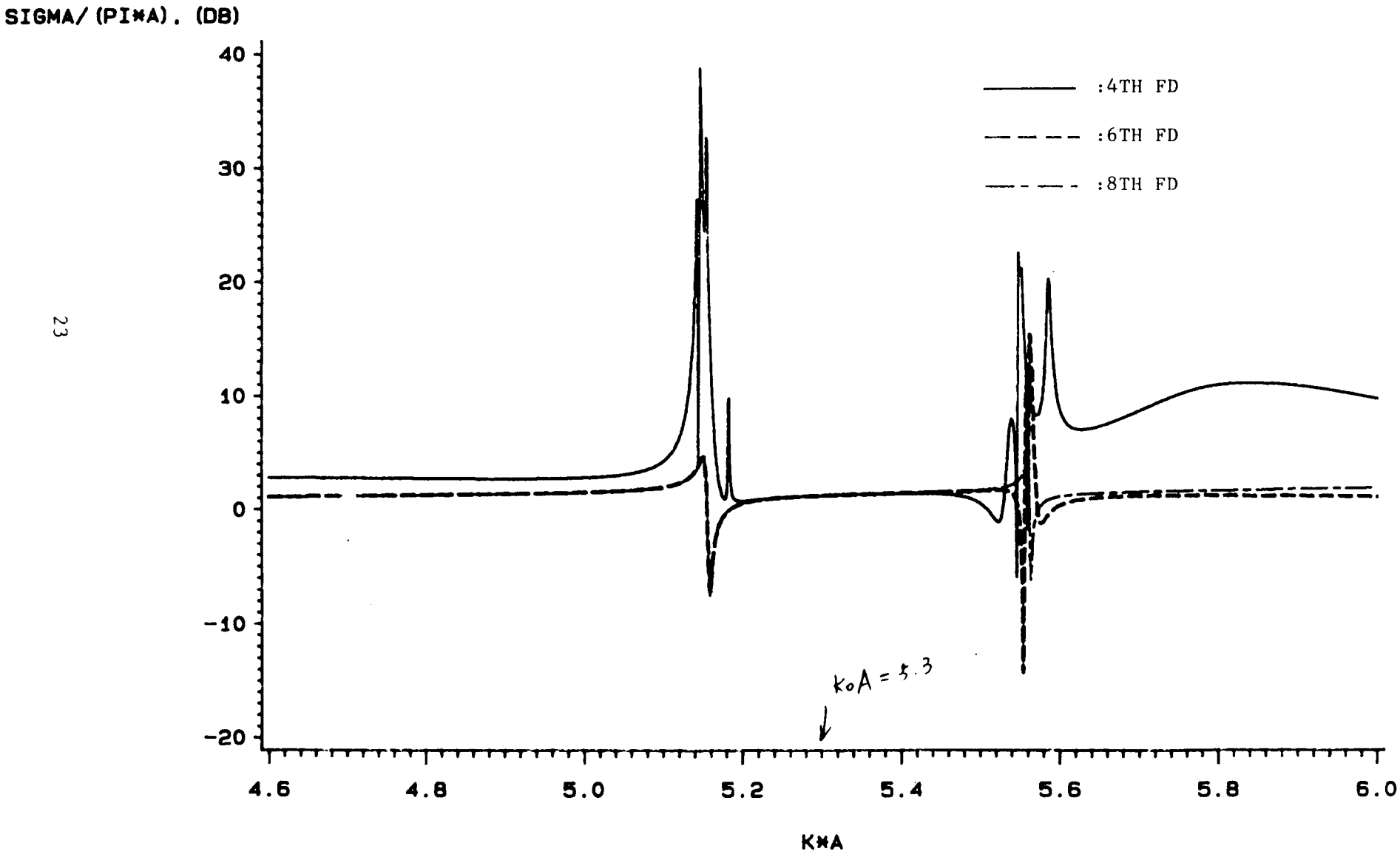
BACKSCATTERING CROSS-SECTION
0 DEG. INCIDENCE
SIGMA/(PI*A). (DB)
40
30
20
10
0
-10
-20
4.6
4.8
5.0
5.2
5.4
5.6
5.8
6.0
K*A
:4TH FD
:6TH FD
:8TH FD
kₒA = 5.3

FIGURE (5)

BACKSCATTERING CROSS-SECTION
0 DEG. INCIDENCE

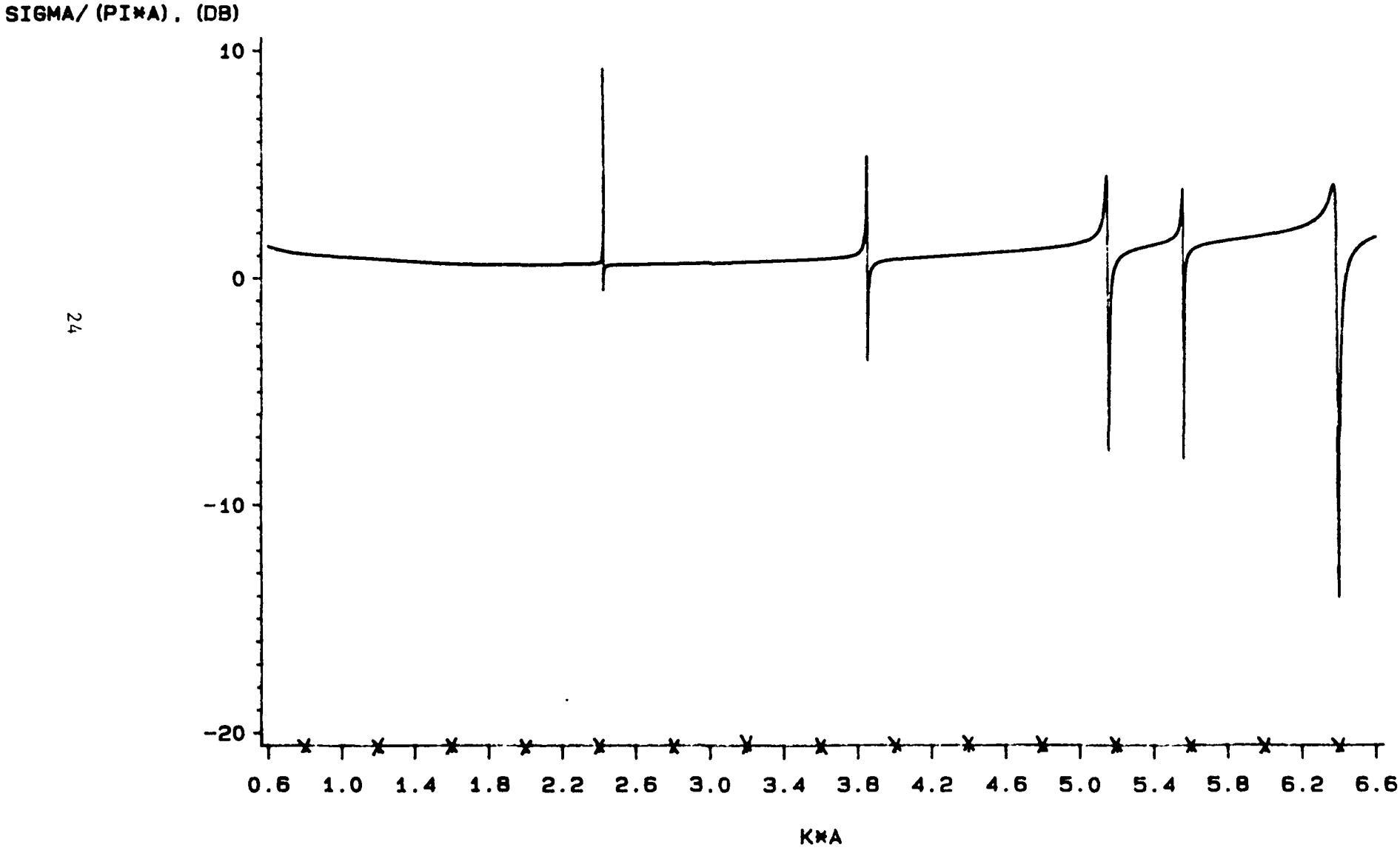

FIGURE (6)

15 6TH FD MODELS

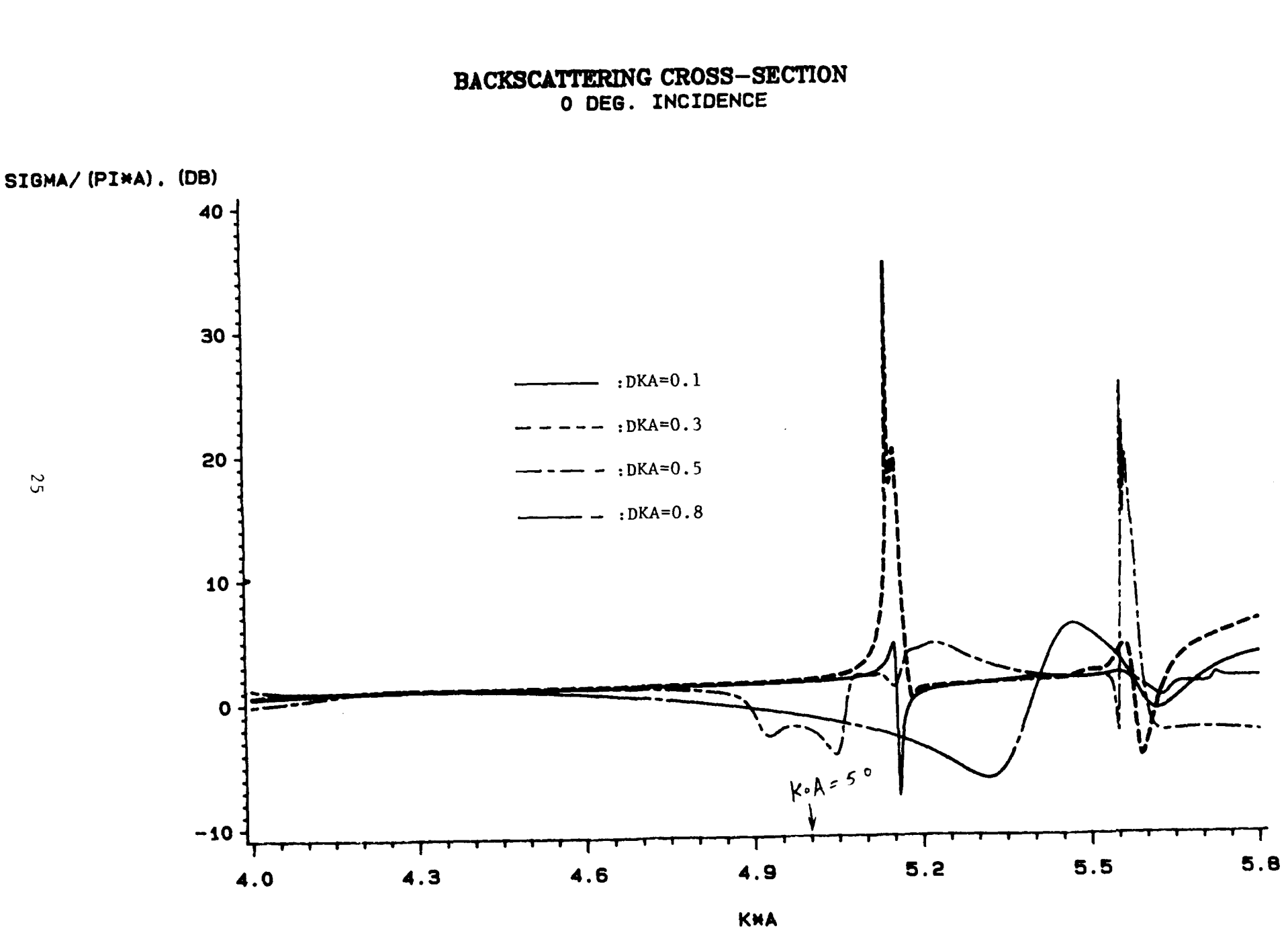
BACKSCATTERING CROSS-SECTION
0 DEG. INCIDENCE
SIGMA/ (PI*A). (DB)
40
30
20
10
0
-10
:DKA=0.1
:DKA=0.3
:DKA=0.5
:DKA=0.8
K◦A = 5°
4.0
4.3
4.6
4.9
5.2
5.5
5.8
K*A

FIGURE (7)

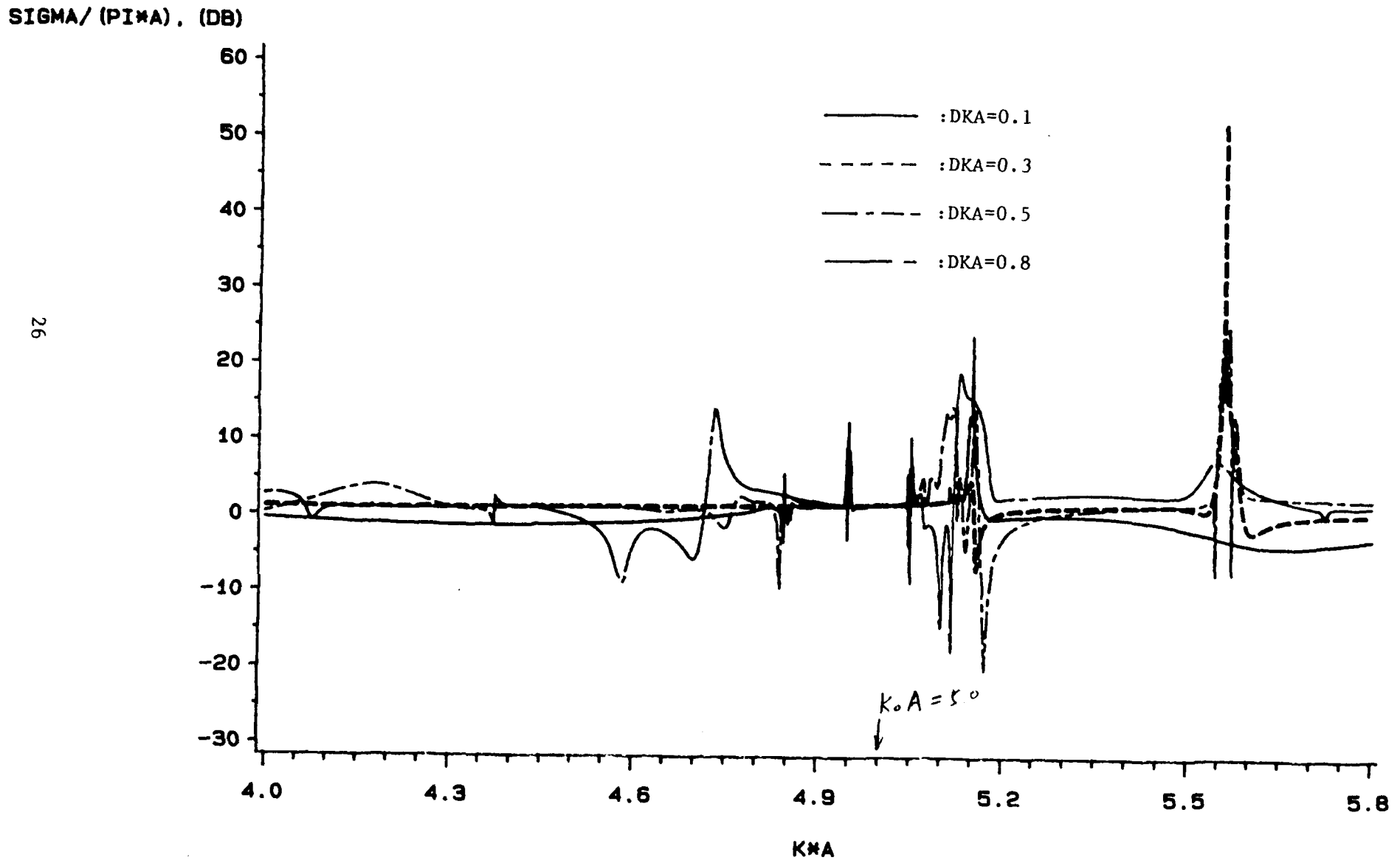
BACKSCATTERING CROSS-SECTION
0 DEG. INCIDENCE
SIGMA/(PI*A), (DB)
60
50
40
30
20
10
0
-10
-20
-30
:DKA=0.1
:DKA=0.3
:DKA=0.5
:DKA=0.8
k₀A = 5
4.0
4.3
4.6
4.9
5.2
5.5
5.8
K*A

FIGURE (6)

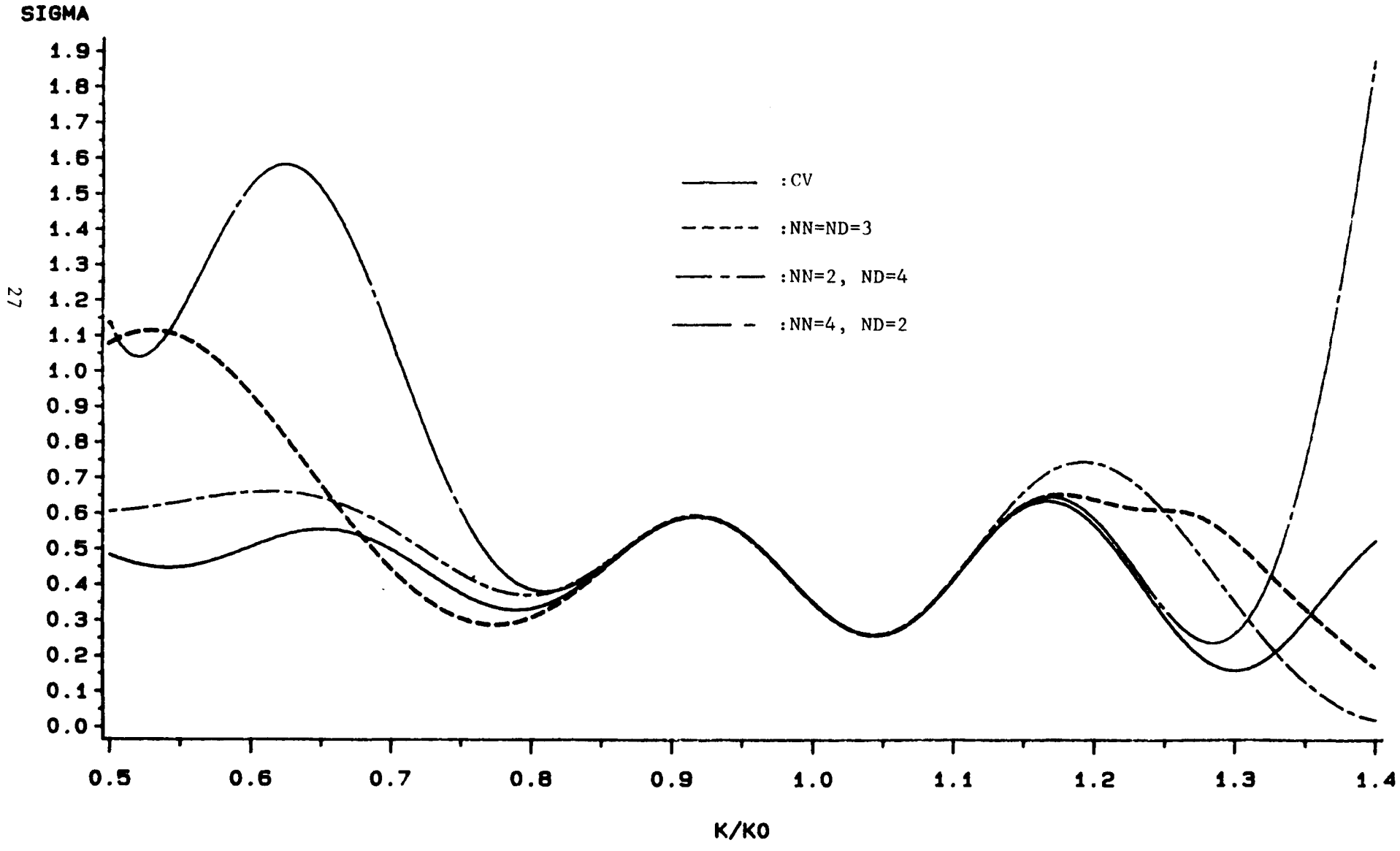
BACKSCATTERING CROSS-SECTION
0 DEG. INCIDENCE
SIGMA
1.9
1.8
1.7
1.6
1.5
1.4
1.3
1.2
1.1
1.0
0.9
0.8
0.7
0.6
0.5
0.4
0.3
0.2
0.1
0.0
:CV
:NN=ND=3
:NN=2, ND=4
:NN=4, ND=2
0.5
0.6
0.7
0.8
0.9
1.0
1.1
1.2
1.3
1.4
K/K0

FIGURE (9)

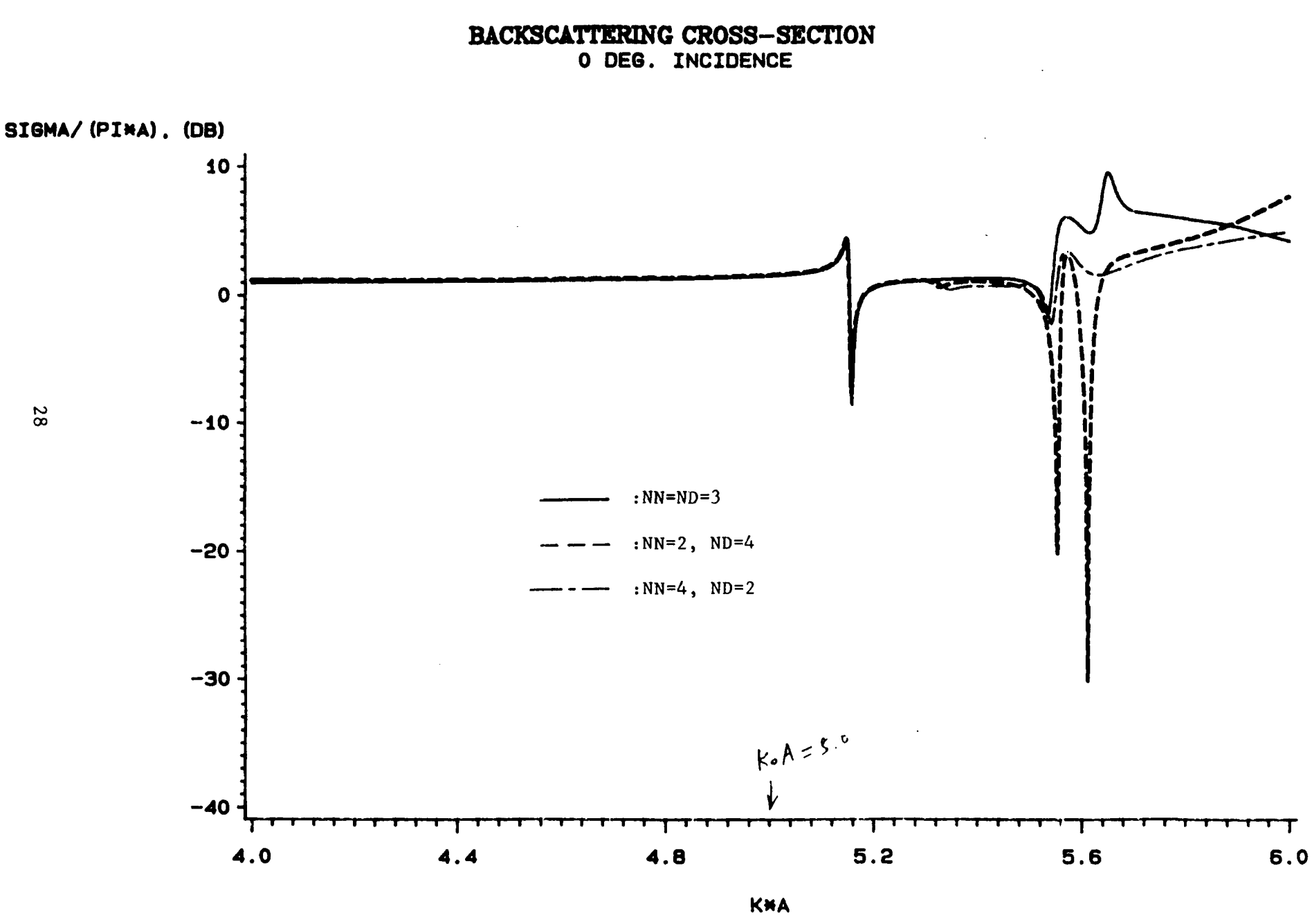
BACKSCATTERING CROSS-SECTION
0 DEG. INCIDENCE
SIGMA/(PI*A). (DB)
10
0
-10
-20
-30
-40
:NN=ND=3
:NN=2, ND=4
:NN=4, ND=2
K₀A = 5.0
4.0
4.4
4.8
5.2
5.6
6.0
K*A

FIGURE (10)